Supporting Information

Hybrid Transition Metal (V, Fe, and Co) Oxide/Sulfide Catalytast for High-efficient Water Electrolysis

Xinwei Wen[a], Xiaoqiang Yang[a], Shuli li[a], Qing Qu[a] and Lei Li[b]**

a* School of Chemical Science and Technology, Yunnan University, Kunming 650091, China

b* State Key Laboratory for Conservation and Utilization of Bio-Resources in Yunnan, Yunnan University, Kunming 650091, China

Experimental method

Materials and chemicals

Ni foam (99.8 wt%, 1 mm in thickness), ferric sulphate hydrate ($FeSO_4·6H_2O$), cobalt sulphate hydrate ($CoSO_4·7H_2O$), L-Cysteine ($C_3H_7NO_2S$), 3 M HCl, ethanol and ammonium vanadate (NH_4VO_3) were purchased from Sinopharm Chemical Reagent Co., Ltd.; cobalt sulphate hydrate ($CoSO_4·7H_2O$), Pt/C (Pt 20%), Nafion (5 wt%) were purchased from Sigma-Aldrich, Ltd. All the reagents were used as received without further purification. Deionized (DI) water was used throughout the experimental processes. Ni foam was used as substrate, after it was ultrasonically washed with 3 M HCl and DI water for 15 minutes, respectively

(1) Preparation of $VCoFe_2O_x$/$VCoFe_2S_x$ catalysts.

Firstly, 1 mmol L-Cysteine was dissolved in 15 mL deionized water and 278.0 mg $FeSO_4·7H_2O$, 140. 1 mg $CoSO_4·7H_2O$ and 116.9 mg NH_4VO_3 dissolved in 15 mL deionized water. Then L-Cysteine solution was quickly added into the solution. Two Ni foams (0.5×2 cm^2) were immersed into ferric sulfate solution and stirred for 15minutes. Poured this mixture into the 50 mL hydrothermal reactor and sealed and reacted at 200 °C for 4 h. After it cooled down, the precipitates and Ni foam were washed three times with anhydrous ethanol and ultrapure water cleaned with DI water and dried overnight at 60℃.

Similarly, $VCoFeO_x$/$VCoFeS_x$ and $VFeO_x$/$VFeS_x$ were synthesized by the changing the proportion of the $CoSO_4·7H_2O$，the other conditions were same with $VCoFe_2Ox$/$VCoFe_2S_x$ catalysts.

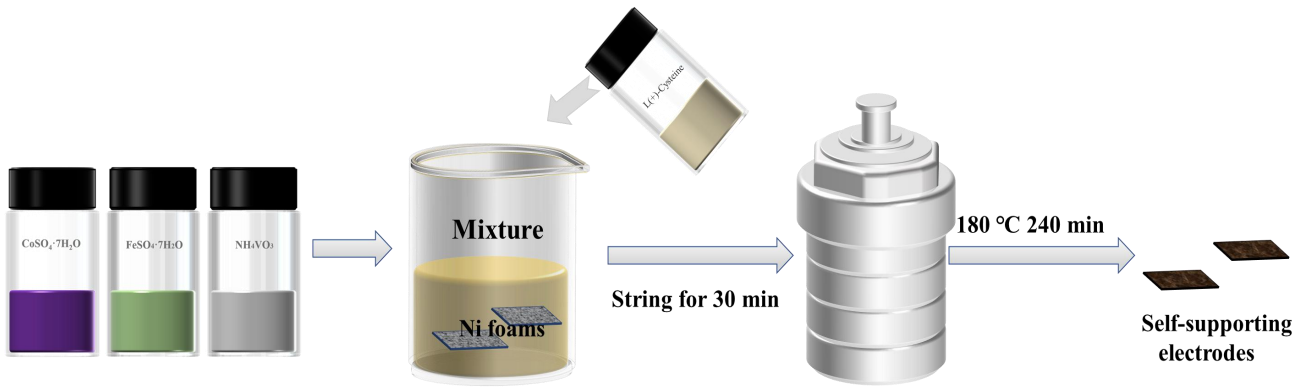

Characterizations

The catalysts were characterized by Bruker D8 advance X-ray diffraction (XRD) with Cu Kα radiation. X-ray photoelectron spectroscopy (XPS) measurement was carried on an ECSALAB-MKII spectrometer with an Al Kα radiation source. The morphology was examined with an FEI Sirion-200 scanning electron microscope (SEM) and a transmission electron microscope (TEM) operating at 200 kV.

Electrochemical Measurements

The electrochemical measurements were performed on a Chie-760 electrochemical workstation at room temperature (25 ºC). The OER and HER performance was measured in a standard three-electrode cell using a Ni foam (NF, 0.25 cm^2) as working electrode while the graphite rod and the saturated calomel electrode (SCE) were used as the counter and reference electrode, the commercial Pt/C and RuO_2 loading to a NF electrode as working electrode. Notably, the SCE was calibrated before and after the tests. The potentials reported in the work were converted to the reversible hydrogen electrode (RHE) by $E_{(RHE)} = E_{(SCE)} + 0.0591 \cdot pH + 0.2412$ V. The equation of $\eta(V) = E_{(RHE)} - E^0$ was used to calculate overpotential of these electrocatalysts, where E^0 represents the thermodynamic potential for OER (1.23 V vs. RHE).

The preparation of the commercial catalyst ink was shown as follows: 5 mg of as-prepared catalysts, 950 μL ethanol and 50 μL Nafion solution were mixed and sonicated for 30 min to make a homogeneous dispersion. Then 5 μL of the catalyst ink was loaded on GC and dried at room temperature. All the data are presented with IR compensation at 85% unless otherwise noted.

Liner Scan Voltammogram Measurements:

Before conducting the electrochemical experiments, the electrolyte was purged by pure N_2 for approximately 30 min. Then the freshly prepared working electrode was immersed in the electrolyte. The liner scan voltammogram (LSV) curves were obtained by sweeping the potential from 0.15 to 0.60 V for OER and -0.95 to -1.40 V for HER (potential vs. SCE) at room temperature, with a sweep rate of 5 mV s^{-1}. Tafel plots were recorded at a scan rate of 5 mV s^{-1} via LSV curves.

Electrochemical double-layer capacitance measurements:

The electrochemically active surface areas (ECSA) were estimated from the electrochemical double-layer capacitance (C_{dl}) by measuring voltammograms at different scan rate in a potential window ranging from 0 V to 0.08 V (0.010 to 0.018 for Ni foam) vs. SCE where no Faradaic process occurred. The ECSA of a catalyst sample is calculated from the double-layer capacitance according to eqation $ECSA = C_{dl} / C_s$.[1] The C_s (80 μF cm^{-2}) is similar to the average areal capacitance in oxide systems.[2]

Chronoamperometry measurements:

To evaluate the stability of OER and HER, the chronoamperometry experiment was carried out in 1 M KOH solutions at 25 mA/cm^2 for OER and at 10 mA/cm^2 for HER for 10 hours. The durability test was carried out for 2000 cycles within the potential ranging from 0.10 to 0.50 V vs. SCE for OER (0.90-1.30V for HER) in 1 M KOH at a scan rate of 50 mV s^{-1}, and a linear sweep was measured under a sweep rate of 5 mV s^{-1} after 2000 cycles.

Electrochemical Impedance Measurements:

The electrochemical impedance spectra (EIS) were recorded at the frequency range from 10 kHz to 0.1 Hz. The amplitude of the sinusoidal potential signal was 5 mV. All the data are presented with R_s deducting unless otherwise noted.

Supporting Figures and Tables

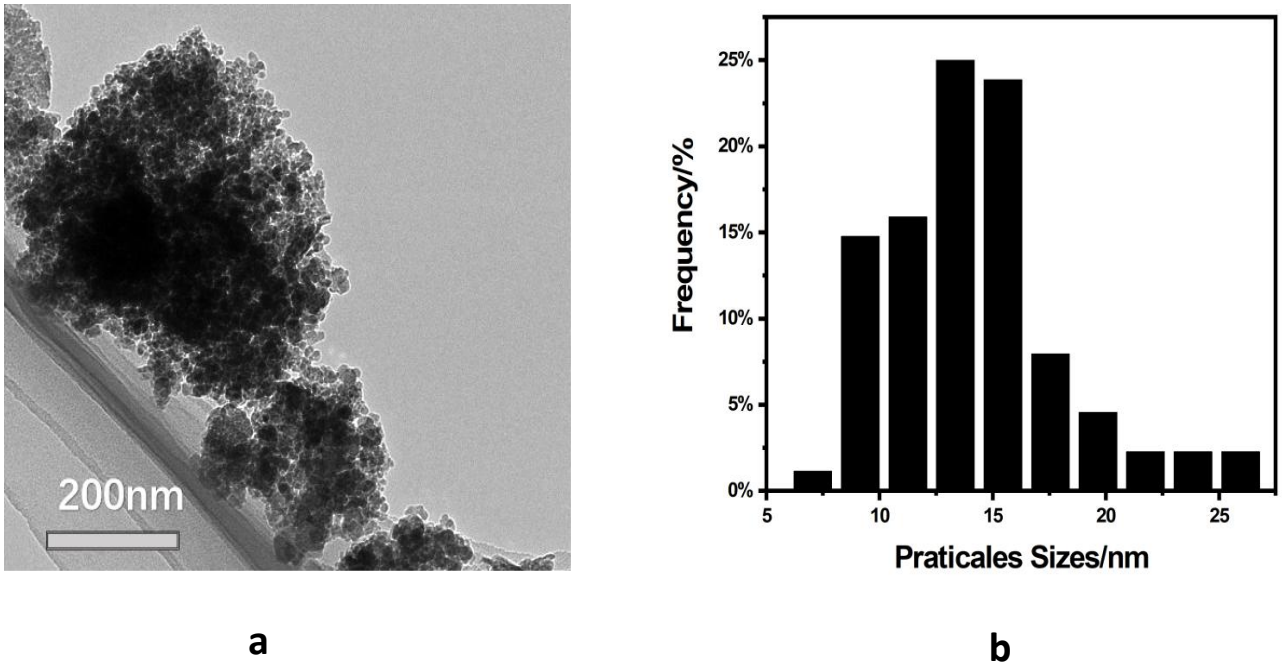

Figure S1. TEM images of the of $VCoFe_2O_x/VCoFe_2S_x$ catalyst (a)， and the particle size distribution histogram of $VCoFe_2O_x/VCoFe_2S_x$ catalyst (b).

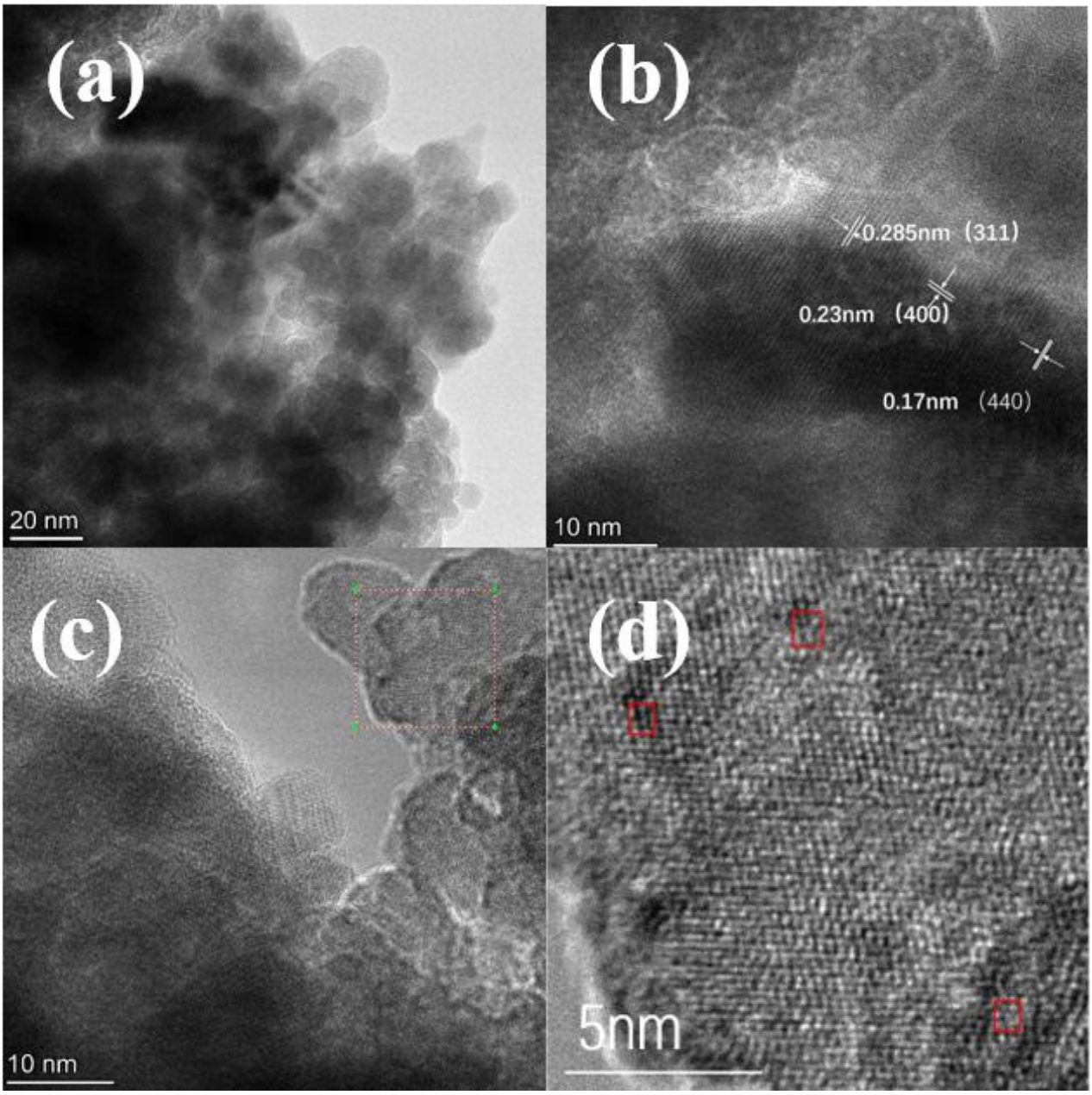

Figure S2. TEM images of the edge of $VCoFe_2O_x/VCoFe_2S_x$ catalyst(a)，(c) ,the TEM images of the lattices of $VCoFe_2O_x/VCoFe_2S_x$ catalyst (b) and the defects of the catalyst in the red boxes (d).

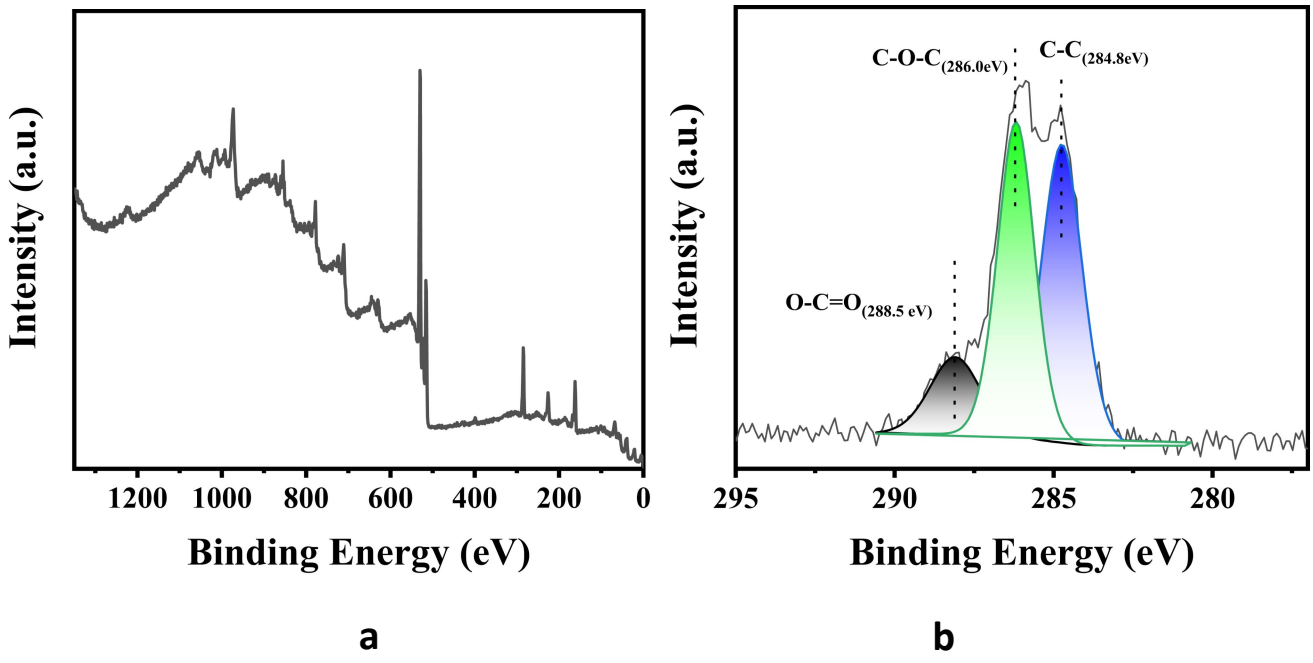

Figure S3. The high-resolution XPS spectra of (a) $VCoFe_2O_x/VCoFe_2S_x$ catalysts and of $VCoFe_2O_x/VCoFe_2S_x$ catalysts in the C 1s region(b).

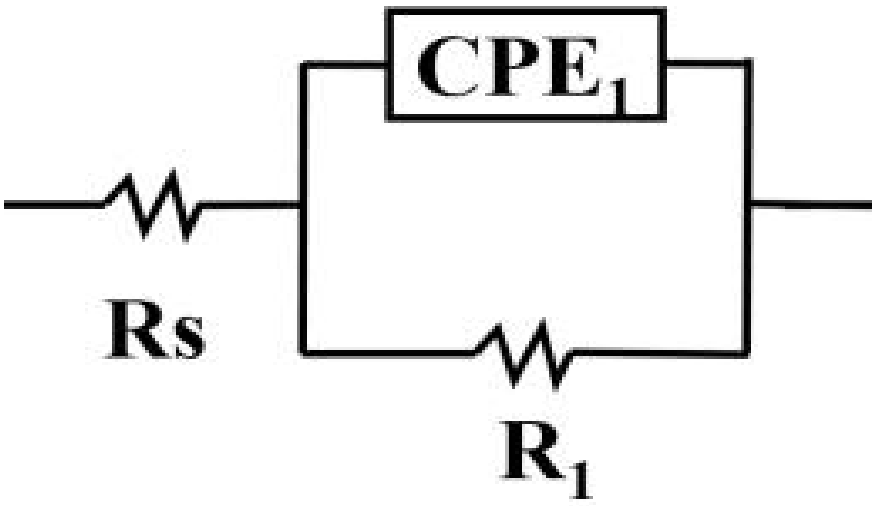

Figure S4. The equivalent circuit model of EIS analysis of all samples.

The equivalent circuit includes a parallel combination of R_{ct} and CPE_1 element in series with R_s. The CPE generally was employed to well fit the impedance data by safely treating as an empirical constant without considering the its physical basis. It was always regarded as the double layer capacitor from the catalyst. R_s was a sign of the uncompensated solution resistance, R_{ct} was a charge transfer resistance arisen from the relevant electro-chemical oxidation.

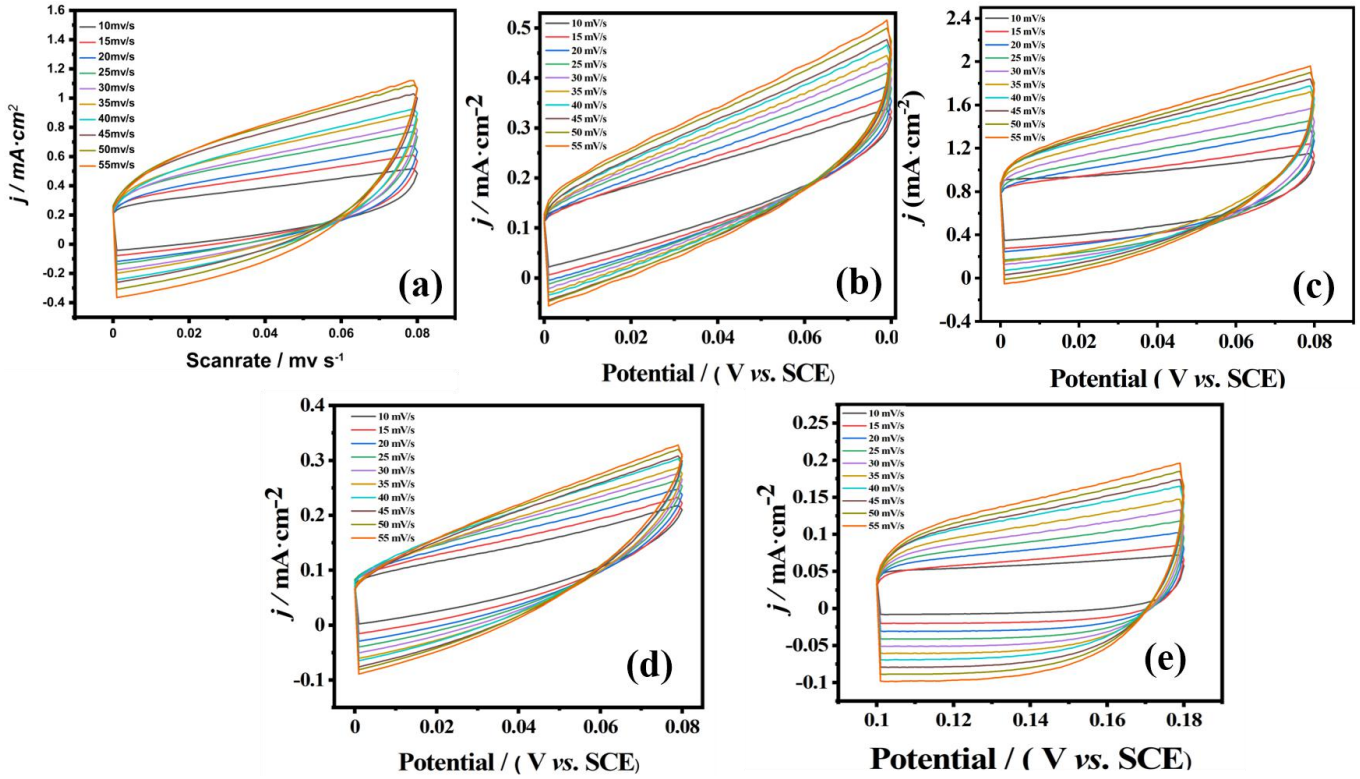

Figure S5. Typical CV curves of catalysts $VCoFe_2O_x/VCoFe_2S_x$ (a); $VCoFeO_x/VCoFeS_x$ (b); $VFeO_x/VFeS_x$ (c); VO_x/VS_x (d); and Ni foam (e); electrodes in 1.0 M KOH with different scan rates.

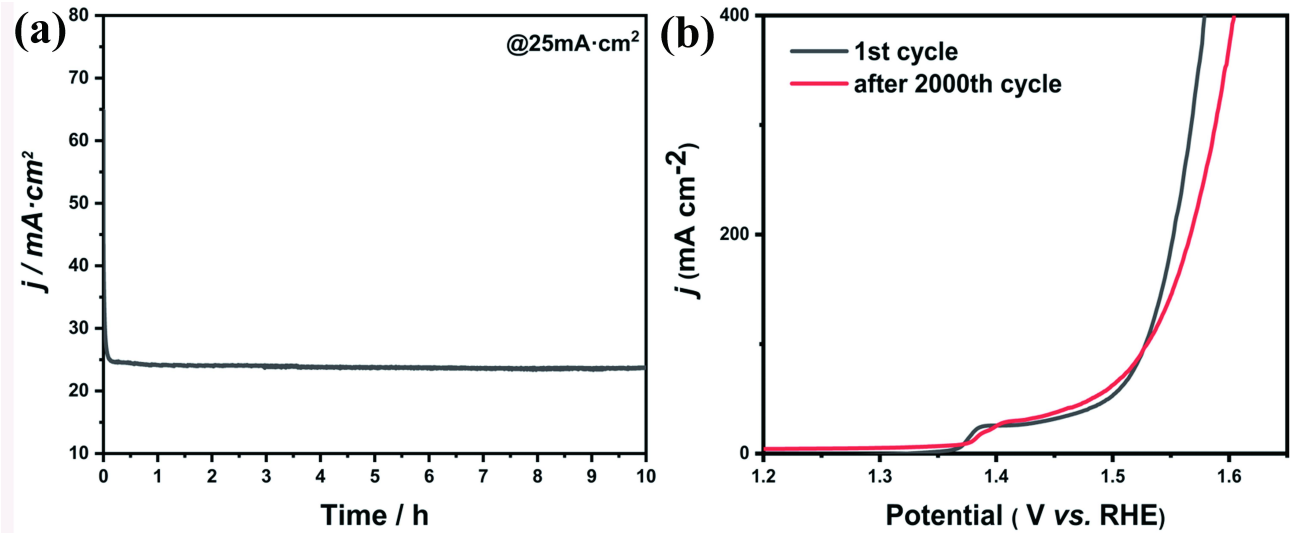

Figure S6. The cycle stability of the $VCoFe_2O_x$/$VCoFe_2S_x$ in OER. I-t curve at 25 mA/cm^2 for OER and the LSV curve after 2000 cycles.

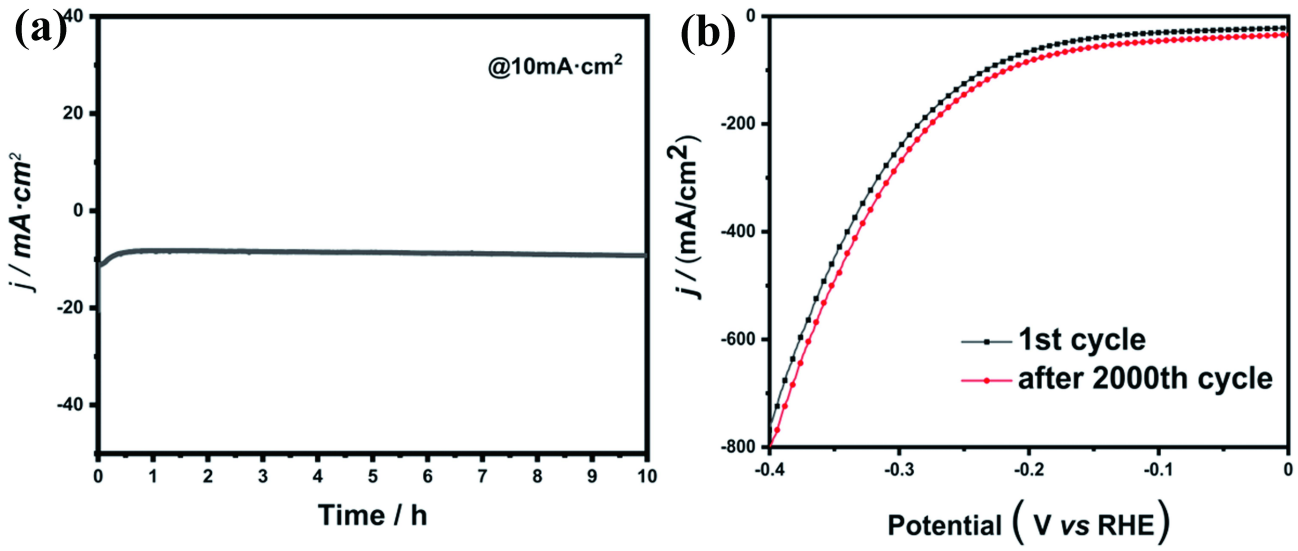

Figure S7. The cycle stability of the $VCoFe_2O_x/VCoFe_2S_x$ in HER. The cycle stability of the $VCoFe_2O_x/VCoFe_2S_x$ in HER. I-t curve at 10 mA/cm^2 and the LSV curve after 2000 cycles.

Table S1. The Inductively Coupled Plasma Optical Emission Spectrometer (ICP-OES) composition of $VCoFe_2O_x/VCoFe_2S_x$ catalyst.

Element	Mass Concentration mg/L	Atomic %
V	32.569	26.52
Co	14.005	10.40
Fe	29.340	20.65
S	38.689	50.03

Table S2. The overpotentials at the current density of 50 mA cm^{-2} (η), Tafel slopes, for electrocatalytic OER and HER tests in 1.0 M KOH

Catalysts	η_{50} for OER	Tafel slope (mV dec^{-1})	η_{50} for HER	Tafel slope (mV dec^{-1})
$VCoFe_2O_x/VFe_2S_x$	267mV	81.42	192mV	91.47
$VCoFeO_x/VCoFeS_x$	313mV	108.01	220mV	153.2
$VFeO_x/VFeS_x$	298mV	173.29	253mV	189.3
RuO_2‖Pt/C	340mV	101.32	89mV	78.48

Table S3. Electrochemical active surface area (ECSA) estimation from C_{dl} experiment catalysts in 1.0 M KOH.

Catalysts	C_{dl}/mF	ECSA /cm^2
$VCoFe_2O_x/VCoFe_2S_x$	34.12	213.25
$VCoFeO_x/VFeS_x$	12.68	79.25
$VFeO_x/VFeS_x$	13.18	82.38
VO_x/VS_x	8.42	52.63
Ni Foam	7.80	48.75

Table S4. Comparison of transition-metal based OER electrocatalysts in alkaline electrolyte.

Catalyst	Electrolyte	OER η_{10} (mV)	Tafel slope (mV/dec)	reference
$NiFe_2O_4$/NF	1.0M KOH	293	98	[3]
FeOOH(Se)/IF	1.0M KOH	287	54	[4]
Co-Ni_3N	1.0M KOH	307	57	[5]
NiFe/NiFeO	1.0M KOH	340	34	[6]
CoV_2O_4	1.0M KOH	370	52	[7]
CoP/MXene	1.0M KOH	230	32.5	[8]
CoP	1.0M KOH	400	80	[9]
CoP-CNT	1.0M KOH	330	50	[9]
CoN/Cu_3N	1.0M KOH	303@50	75.7	[10]
CoS–NiS	1.0M KOH	281@50	53.3	[11]
NiS	1.0M KOH	335@50	153	[12]
$VCoFeO_x/VFeS_x$	1.0M KOH	313@50	108.01	This work
$VCoFe_2O_x/VFe_2S_x$	1.0M KOH	267@50	33.25	This work

Table S5. Comparison of overall water splitting activities of bifunctional electrocatalysts with high current at 500 mA cm^{-2}.

Catalyst	Electrolyte	Potential@10mA/cm^2	reference
Ni_3S_2	1.0M KOH	1.76V	[13]
$NiCo_2S_4$	1.0M KOH	1.68 V	[14]
$NiCo_2Px$/CNTs	1.0M KOH	1.61V	[15]
$Co_2P/Mo_2C/Mo_3Co_3C$@C	1.0M KOH	1.74V	[16]
$CoO/CoSe_2$	1.0M KOH	2.18V	[17]
Co–P/NC	1.0M KOH	1.55V	[18]
CoS_2 NTA/CC	1.0M KOH	1.67V	[19]
Co_9S_8–NSC@Mo_2C	0.5M H_2SO_4	1.61V	[20]
Co3S4/EC–MOF	1.0 M KOH	1.55V	[21]
CoFe/NF	1.0 M KOH	1.64V	[22]
$VCoFe_2O_x/VFe_2S_x$	1.0 M KOH	1.58V@10 1.72V@50	This work

Table S6. EIS fitting parameters from equivalent circuits for different catalysts in the 1 M KOH solution.

Catalyst	R_{CT} for OER/ Ω	R_{CT} for HER/ Ω
$VCoFe_2O_x/VFe_2S_x$	3.0	5.81
$VCoFeO_x/VCoFeS_x$	14.3	11.7
$VFeO_x/VFeS_x$	6.8	19.5
RuO_2‖Pt/C	37.9	2.1
Ni Foam	107.4	57.1

Reference

1. C. C. L. McCrory, S. Jung, J. C. Peters and T. F. Jaramillo, *Journal of the American Chemical Society*, 2013, **135**, 16977-16987.
2. M. B. Stevens, L. J. Enman, A. S. Batchellor, M. R. Cosby, A. E. Vise, C. D. M. Trang and S. W. Boettcher, *Chemistry of Materials*, 2017, **29**, 120-140.
3. Z. Fang, Z. Hao, Q. Dong and Y. Cui, *Journal of Nanoparticle Research*, 2018, **20**, 106.
4. S. Niu, W.-J. Jiang, Z. Wei, T. Tang, J. Ma, J.-S. Hu and L.-J. Wan, *Journal of the American Chemical Society*, 2019, **141**, 7005-7013.
5. C. Zhu, A. L. Wang, W. Xiao, D. Chao and H. J. Fan, *Advanced Materials*, 2018, **30**, e1705516.
6. K. Zhu, M. Li, X. Li, X. Zhu, J. Wang and W. Yang, *Chemical Communications*, 2016, **52**, 11803-11806.
7. S. E. Michaud, M. T. Riehs, W.-J. Feng, C.-C. Lin and C. C. L. McCrory, *Chemical Communications*, 2021, **57**, 883-886.
8. S. Hirai, K. Morita, K. Yasuoka, T. Shibuya, Y. Tojo, Y. Kamihara, A. Miura, H. Suzuki, T. Ohno, T. Matsuda and S. Yagi, *Journal of Materials Chemistry A*, 2018, **6**, 15102-15109.
9. C.-C. Hou, S. Cao, W.-F. Fu and Y. Chen, *ACS Applied Materials & Interfaces*, 2015, **7**, 28412-28419.
10. J. Li, X. Kong, M. Jiang and X. Lei, *Inorganic Chemistry Frontiers*, 2018, **5**, 2906-2913.
11. J. Li, P. Xu, R. Zhou, R. Li, L. Qiu, S. P. Jiang and D. Yuan, *Electrochimica Acta*, 2019, **299**, 152-162.
12. M.-R. Gao, X. Cao, Q. Gao, Y.-F. Xu, Y.-R. Zheng, J. Jiang and S.-H. Yu, *ACS Nano*, 2014, **8**, 3970-3978.
13. L. L. Feng, G. Yu, Y. Wu, G. D. Li, H. Li, Y. Sun, T. Asefa, W. Chen and X. Zou, *Journal of the American Chemical Society*, 2015, **137**, 14023-14026.
14. A. Sivanantham, P. Ganesan and S. Shanmugam, *Advanced Functional Materials*, 2016.
15. C. Huang, T. Ouyang, Y. Zou, N. Li and Z.-Q. Liu, *Journal of Materials Chemistry A*, 2018, **6**, 7420-7427.
16. X. Li, X. Wang, J. Zhou, L. Han, C. Sun, Q. Wang and Z. Su, *Journal of Materials Chemistry A*, 2018, **6**, 5789-5796.
17. K. Li, J. Zhang, R. Wu, Y. Yu and B. Zhang, *Advanced Science*, 2016, **3**, 1500426.
18. B. You, N. Jiang, M. Sheng, S. Gul, J. Yano and Y. Sun, *Chemistry of Materials*, 2015, **27**, 7636-7642.
19. K. Jayaramulu, J. Masa, O. Tomanec, D. Peeters, V. Ranc, A. Schneemann, R. Zboril, W. Schuhmann and R. A. Fischer, *Advanced Functional Materials*, 2017, **27**, 1700451.
20. X. Luo, Q. Zhou, S. Du, J. Li, J. Zhong, X. Deng and Y. Liu, *ACS Applied Materials & Interfaces*, 2018, **10**, 22291-22302.
21. T. Liu, P. Li, N. Yao, T. Kong, G. Cheng, S. Chen and W. Luo, *Advanced Materials*, 2019, **31**, 1806672.
22. P. Babar, A. Lokhande, H. H. Shin, B. Pawar, M. G. Gang, S. Pawar and J. H. Kim, *Small*, 2018, **14**, 1702568.